

Projection based fuzzy least squares twin support vector machine for class imbalance problems

M. Tanveer^{a,*}, Ritik Mishra^a, Bharat Richhariya^b

^a*Department of Mathematics, Indian Institute of Technology Indore, Simrol, Indore
452552, India*

^b*Department of Computer Science & Information Systems, BITS Pilani (Pilani
Campus), India*

Abstract

Class imbalance is a major problem in many real world classification tasks. Due to the imbalance in the number of samples, the support vector machine (SVM) classifier gets biased toward the majority class. Furthermore, these samples are often observed with a certain degree of noise. Therefore, to remove these problems we propose a novel fuzzy based approach to deal with class imbalanced as well noisy datasets. We propose two approaches to address these problems. The first approach is based on the intuitionistic fuzzy membership, termed as robust energy-based intuitionistic fuzzy least squares twin support vector machine (IF-RELSTSVM). Furthermore, we introduce the concept of hyperplane-based fuzzy membership in our second approach, where the final classifier is termed as robust energy-based fuzzy least square twin support vector machine (F-RELSTSVM). By using this technique, the membership values are based on a projection based approach, where the data points are projected on the hyperplanes. The performance of the proposed algorithms is evaluated on several benchmark and synthetic datasets. The experimental results show that the proposed IF-RELSTSVM and F-RELSTSVM models outperform the baseline algorithms. Statistical tests are performed to check the significance of the proposed algorithms. The results show the applicability of the proposed algorithms on noisy as well as imbalanced datasets.

Keywords: Projection based membership, Intuitionistic fuzzy set, Energy parameters, Class imbalanced noisy data, Least squares method.

*Corresponding author

1. Introduction

Support vector machines (SVMs) [1] are computationally powerful tools for supervised learning, and therefore frequently utilized in classification [2] and regression problems [3]. SVMs have been effectively used to solve a range of real world problems, including intrusion detection system [4], facial expression recognition [5], speaker identification [6], text classification [7], and seizure detection [8]. The methodical approach of SVMs is driven by the statistical learning theory. Finding the best-separating hyperplane between the positive and negative instances is the main goal of SVM. However, despite their effectiveness, SVMs have some limitations, such as higher time complexity, sensitivity to noise and outliers, and inability to handle class imbalance problems [9].

To address the limitations mentioned above, several variants of SVM have been proposed, such as generalized eigenvalue problem-based SVM (GEPSVM) [10] and fuzzy support vector machine (FSVM) [11]. GEPSVM solves a generalized eigenvalue problem which is computationally efficient and provides a better solution than SVM. Jayadeva et al. [11] proposed a twin support vector machine (TWSVM) that constructs two non-parallel hyperplanes like GEPSVM. However, unlike GEPSVM, TWSVM solves a pair of smaller-sized quadratic programming problems (QPPs) instead of a generalized eigenvalue problem. TWSVM is efficient with respect to time complexity in comparison to SVM. To reduce the computational complexity of TWSVM, the least squares twin support vector machine (LSTSVM) [12] was proposed as an alternative to the convex QPPs in TWSVM. LSTSVM utilizes the squared loss function instead of the hinge loss function, resulting in lower training time [13]. However, the LSTSVM model needs the hyperplane at exactly one distance from the other class, making it sensitive to noise and outliers.

To address the sensitivity to noise near the hyperplanes, Nasiri et al. [14] developed the energy-based LSTSVM (ELS-TSVM) model, which introduces energy parameters to relax the constraints for the hyperplanes. Furthermore, Tanveer et al. [15] developed a robust energy-based least square twin support vector machine (RELS-TSVM) by incorporating regularization terms in ELS-TSVM, making it more robust to noise. Recent studies have shown that the RELS-TSVM model and its variants outperform other TWSVM-based

models in binary class problems because they can handle noise and outliers effectively [16]. Recently, Laxmi et al. [17] suggested another TWSVM variant, intuitionistic fuzzy least square twin support vector machine (IFLSTSVM). IFLSTSVM incorporates the concept of the intuitionistic fuzzy set [18], which handles the uncertainties in the data more precisely.

One of the frequently encountered problems in real world classification tasks is class imbalance [19, 20, 21]. In case of RELS-TSVM, the classifier gives equal weightage to each sample, causing the learned decision surface to get biased toward the majority class. To address this issue, we propose two improved variants of RELS-TSVM algorithm, known as robust energy-based intuitionistic fuzzy least squares twin support vector machine (IF-RELSTSVM) and robust energy-based fuzzy least squares twin support vector machine (F-RELSTSVM) for class imbalance learning. Unlike TWSVM, LSTSVM, ELS-TSVM, and RELS-TSVM models, the proposed IF-RELSTSVM introduces intuitionistic fuzzy scores to both classes to reduce the negative effect of noise and outliers. This intuitionistic fuzzy score is achieved by introducing a pair of membership and non-membership degrees for every data point. The proposed IF-RELSTSVM model also incorporates a regularization term to reduce over-fitting. This extra component encapsulates the marrow of statistical learning theory and implements the structural risk minimization (SRM) principle in the proposed formulation.

Furthermore, in the proposed F-RELSTSVM model, we present another approach where the projection on proximal hyperplanes is utilized for the fuzzy memberships. Both the proposed IF-RELSTSVM and F-RELSTSVM models solve systems of linear equations instead of QPPs as in TWSVM. Therefore, the proposed models are robust compared to the TWSVM, LSTSVM, and ELS-TSVM. Moreover, the proposed models can handle the class imbalance problem by introducing a weight parameter to the objective function, which balances the influence of the minority and majority classes in the learning process. To evaluate the performance of the proposed algorithms, we conducted experiments on several benchmark datasets. Experimental results show that the performance of the proposed F-RELSTSVM model is better than other state-of-the-art algorithms, including LSTSVM, ELS-TSVM, RELS-TSVM, and IFLSTSVM in terms of AUC [22].

The proposed IF-RELSTSVM and F-RELSTSVM models have the following appealing features:

1. Unlike TWSVM, LSTSVM, ELS-TSVM, and RELS-TSVM, the pro-

posed IF-RELSTSVM model introduces intuitionistic fuzzy score to both classes that reduce the effect of noise and outliers in samples. IF-RELSTSVM introduces a pair of membership and non-membership degrees for every data point. Moreover, the membership degree uses the imbalance ratio (IR) as a multiplier to deal with class imbalance issues in the datasets. So, the problems of class imbalance and noisy data are handled in this approach.

2. The proposed IF-RELSTSVM algorithm provides solution to two types of noise:
 - (a) Noise near the hyperplane which is dealt with energy-based approach.
 - (b) Noise away from the hyperplane which is dealt with the intuitionistic fuzzy-based approach in this work.
3. The proposed F-RELSTSVM model utilizes the projection on proximal hyperplanes to measure the membership leading to proper fuzzy memberships to the data points before formulating the final classifier.
4. IF-RELSTSVM and F-RELSTSVM involve the regularisation term to each objective function to maximize the margin. This involves the structural risk minimization principle in the proposed formulations.
5. The proposed formulations involve the solution of system of linear equations instead of QPPs, leading to lesser computation time.

2. Related work

This section discusses the intuitionistic fuzzy set and formulations of LSTSVM, ELS-TSVM, and RELS-TSVM algorithms.

Suppose $X = \{(x_1, y_1), (x_2, y_2), \dots, (x_m, y_m)\}$ is a set of training samples, where $x_l \in \mathbb{R}^n$ being the l^{th} training sample, $l \in \{1, 2, \dots, m\}$ and $y_i \in \{-1, +1\}$ being the associated target class.

2.1. Intuitionistic fuzzy set

Let A be a nonempty set. A fuzzy set [23] F in the universe A is defined by

$$F = \{(y, \mu_F(y)) : y \in A\},$$

where, $\mu_F : X \rightarrow [0, 1]$ is the membership (degree of belongingness) of y to A .

Intuitionistic fuzzy (IF) set [18] can be defined as

$$IF = \{(y, \mu_{IF}(y), \eta_{IF}(y)) : y \in A\},$$

where $\mu_{IF} : X \rightarrow [0, 1], \eta_{IF} : X \rightarrow [0, 1], 0 \leq \mu_{IF}(y) + \eta_{IF}(y) \leq 1$, μ_{IF} and η_{IF} represent the membership and non-membership degrees of belongingness of y in A , respectively.

For a data point y , the degree for not belonging to A is defined by

$$h_{IF}(y) = 1 - \mu_{IF}(y) - \eta_{IF}(y).$$

An intuitionistic fuzzy number (IFN) is defined by

$$IFN = (\mu_{IF}, \eta_{IF}).$$

Hence, $(1, 0)$ represents the highest membership value and least non-membership value, while $(0, 1)$ represents the least membership value and the highest non-membership value. Therefore, the largest intuitionistic fuzzy number and smallest intuitionistic fuzzy numbers are $(1, 0)$ and $(0, 1)$, respectively. For a given IFN the score value is given as

$$s(IFN) = \mu_{IFN} - \eta_{IFN}.$$

Similarly, another precise score value [24] can be defined as

$$\begin{aligned} p(IFN) &= \mu_{IFN} + \eta_{IFN}, \\ \therefore p(IFN) + h_{IF}(IFN) &= 1. \end{aligned}$$

For given IFN_1 and IFN_2 , we can say that $IFN_1 < IFN_2$ if

$$s(IFN_1) = s(IFN_2) \text{ and } p(IFN_1) < p(IFN_2).$$

Here, we define a derived score using the precise score values as

$$K(IFN) = \frac{1 - \eta_{IFN}}{2 - \mu_{IFN} - \eta_{IFN}}.$$

Thus, there is conjunction between membership and non-membership values as follows:

$$1. \ s(IFN_1) < s(IFN_2) \Rightarrow K(IFN_1) < K(IFN_2),$$

$$2. \ s(IFN_1) = s(IFN_2), p(IFN_1) < p(IFN_2) \Rightarrow K(IFN_1) < K(IFN_2).$$

2.2. Least squares twin support vector machine (LSTSVM)

To minimize the computational complexity of TWSVM, Kumar and Gopal [12] introduced a least squares twin support vector machine (LSTSVM). LSTSVM involves solving a pair of linear equations to obtain two hyperplanes. The formulation of LSTSVM is as follows:

For the binary classification problem, we consider two matrices A and B , consisting of data points with class labels '+1' and '-1' respectively. The dimensions of matrices A and B are $p \times n$ and $q \times n$ respectively, where n is the number of features. Then, the optimization problem of linear LSTSVM is formulated as follows:

$$\begin{aligned} \min_{w_1, b_1, \xi_2} \quad & \frac{1}{2} \|Aw_1 + e_1b_1\|^2 + C_1\xi_2^T\xi_2 \\ \text{subject to} \quad & -(Bw_1 + e_2b_1) + \xi_2 = e_2, \end{aligned} \quad (1)$$

and

$$\begin{aligned} \min_{w_2, b_2, \xi_1} \quad & \frac{1}{2} \|Bw_2 + e_2b_2\|^2 + C_2\xi_1^T\xi_1 \\ \text{subject to} \quad & (Aw_2 + e_1b_2) + \xi_1 = e_1. \end{aligned} \quad (2)$$

After putting the equality constraints in the objective function (1), we get

$$\min_{w_1, b_1} \frac{1}{2} \|Aw_1 + e_1b_1\|^2 + \frac{C_1}{2} \|Bw_1 + e_1b_1 + e_2\|^2. \quad (3)$$

Setting the gradient of (3) with respect to w_1, b_1 and then equating it to zero, we get:

$$A^T(Aw_1 + e_1b_1) + C_1B^T(Bw_1 + e_2b_1 + e_2) = 0, \quad (4)$$

$$e_1^T(Aw_1 + e_1b_1) + C_1e_2^T(Bw_1 + e_2b_1 + e_2) = 0. \quad (5)$$

Defining $G = [A \ e_1]$ and $H = [B \ e_2]$, the solution becomes:

$$\begin{bmatrix} w_1 \\ b_1 \end{bmatrix} = - \left(H^T H + \frac{1}{C_1} G^T G \right)^{-1} H^T e_2. \quad (6)$$

Similarly, the solution of QPP (2) can be shown as,

$$\begin{bmatrix} w_2 \\ b_2 \end{bmatrix} = \left(G^T G + \frac{1}{C_2} H^T H \right)^{-1} G^T e_1. \quad (7)$$

To decrease the computational time required for inverting matrices, the Sherman-Morrison-Woodbury (SMW) formula [25] is employed to solve equation (6) and (7) by finding the inverses of smaller dimension. A new data point $x \in \mathbb{R}^n$ is assigned to a class using the following decision function:

$$\text{class label}(x) = \arg \min_{i \in 1,2} \frac{|w_i^T x + b_i|}{\|w_i\|}. \quad (8)$$

where $| \cdot |$ represents the perpendicular distance between a data point and hyperplane.

2.3. Energy-based least squares twin support vector machine (ELS-TSVM)

To reduce the sensitivity of LSTSVM algorithm to noise and outliers, Nasiri et al. [14] proposed an energy-based least square twin support vector machine that incorporates an energy parameter for each hyperplane to limit the effect of noise and outliers. The optimization problem of ELS-TSVM is defined as:

$$\begin{aligned} \min_{w_1, b_1, \xi_2} \quad & \frac{1}{2} \|Aw_1 + e_1 b_1\|^2 + C_1 \xi_2^T \xi_2 \\ \text{subject to} \quad & -(Bw_1 + e_2 b_1) + \xi_2 = E_2, \end{aligned} \quad (9)$$

and

$$\begin{aligned} \min_{w_2, b_2, \xi_1} \quad & \frac{1}{2} \|Bw_2 + e_2 b_2\|^2 + C_2 \xi_1^T \xi_1 \\ \text{subject to} \quad & (Aw_2 + e_1 b_2) + \xi_1 = E_1, \end{aligned} \quad (10)$$

where C_1, C_2 are positive integers and E_1, E_2 are energy parameters.

On substituting the equality constraints into the objective function of QPP (9), we get:

$$L_1 = \frac{1}{2} \|Aw_1 + e_1 b_1\|^2 + \frac{C_1}{2} \|Bw_1 + e_2 b_1 + E_1\|^2. \quad (11)$$

Setting the gradient of (11) with respect to w_1 and b_1 and equating to zero, the solution of QPP (9) is obtained as follows:

$$\begin{bmatrix} w_1 \\ b_1 \end{bmatrix} = - (C_1 H^T H + G^T G)^{-1} C_1 H^T E_1, \quad (12)$$

where $G = [A \ e_1]$ and $H = [B \ e_2]$. Similarly, we get the solution of QPP (10) as follows:

$$\begin{bmatrix} w_2 \\ b_2 \end{bmatrix} = (C_2 G^T G + H^T H)^{-1} C_2 G^T E_2. \quad (13)$$

A new sample x is assigned depending on the following decision function:

$$\text{class label}(x) = \begin{cases} +1, & \frac{|w_1^T x + b_1|}{|w_2^T x + b_2|} \leq 1, \\ -1, & \frac{|w_1^T x + b_1|}{|w_2^T x + b_2|} > 1, \end{cases} \quad (14)$$

2.3.1. ELS-TSVM vs LSTSVM algorithm

In this section, we compare ELS-TSVM with the LSTSVM algorithm.

1. The LSTSVM algorithm constraints demand the hyperplane to be exactly one distance from the points of the opposite class, making LSTSVM sensitive to outliers. For each hyperplane, ELS-TSVM includes an energy parameter that limits the impact of noise and outliers, and various energy values are chosen depending on past information or the grid search technique.
2. The ELS-TSVM decision function is attained by using primal problems. However, the decision function in LSTSVM is computed using the perpendicular distance.
3. The ELS-TSVM and LSTSVM algorithms are least squares variants of TWSVM that solve linear systems instead of solving the convex QPPs. As a result, ELS-TSVM and LSTSVM algorithms are much faster than TWSVM and have better generalization performance.

2.4. Robust energy-based least squares twin support vector machine (RELS-TSVM)

By incorporating the regularization terms in the optimization of the ELS-TSVM algorithm, the linear case of RELS-TSVM [15] is formulated by the

following pair of QPPs:

$$\begin{aligned} \min_{w_1, b_1, \xi_2} \quad & \frac{1}{2} \|Aw_1 + e_1 b_1\|^2 + C_1 \xi_2^T \xi_2 + \frac{1}{2} C_3 (\|w_1\|^2 + b_1^2) \\ \text{subject to} \quad & -(Bw_1 + e_2 b_1) + \xi_2 = E_2, \end{aligned} \quad (15)$$

and

$$\begin{aligned} \min_{w_2, b_2, \xi_1} \quad & \frac{1}{2} \|Bw_2 + e_2 b_2\|^2 + C_2 \xi_1^T \xi_1 + \frac{1}{2} C_4 (\|w_2\|^2 + b_2^2) \\ \text{subject to} \quad & (Aw_2 + e_1 b_2) + \xi_1 = E_1. \end{aligned} \quad (16)$$

Substituting equality constraints into the objective function, we get the solution for QPP (15).

Let $P = [A \ e_1]$ and $Q = [B \ e_2]$. Then the solution of QPP (15) is given as:

$$\begin{bmatrix} w_1 \\ b_1 \end{bmatrix} = -(P^T P + C_1 Q^T Q + C_3 I)^{-1} C_3 Q^T E_2. \quad (17)$$

In a similar way, the solution for QPP (16) is given by

$$\begin{bmatrix} w_2 \\ b_2 \end{bmatrix} = (Q^T Q + C_2 P^T P + C_4 I)^{-1} C_4 P^T E_1. \quad (18)$$

To reduce the computational time required for inverting matrices, the SMW formula [25] is employed to solve equations (17) and (18). A new sample x is assigned to a class using equation (14).

2.5. Intuitionistic fuzzy membership assignment (IFMA)

In intuitionistic fuzzy membership assignment [24], we employ a score value based on a pair of membership degrees and non-membership degrees to reduce the effect of noise and outliers. In IFMA, the membership degree is calculated in the feature space.

2.5.1. Membership degree

To determine the membership degree of the training data points, we first project the training points in the higher dimensional space. Then, we find the center of both classes and calculate the distance for each training point

from its class center to determine the membership values. Given a training data point x_i one can assign the membership value as:

$$\mu(x_i) = \begin{cases} 1 - \frac{\|\phi(x_i) - C^+\|}{r^+ + \delta}, & y_i = +1, \\ 1 - \frac{\|\phi(x_i) - C^-\|}{r^- + \delta}, & y_i = -1. \end{cases} \quad (19)$$

In equation (19), $C^+(C^-)$ and $r^+(r^-)$ are the center and radius of the class of the positive (negative) class $\delta > 0$ is a small and adjustable parameter, and $\|\cdot\|$ denotes the Frobenius norm.

$$D(\phi(x_i), \phi(x_j)) = \|\phi(x_i) - \phi(x_j)\|, \quad (20)$$

where ϕ maps the input data point into the higher dimensional space. One can calculate the center of class as

$$C^\pm = \frac{1}{l_\pm} \sum_{y_i = \pm 1} \phi(x_i), \quad (21)$$

where l_\pm is the cardinality of samples of positive (negative) class. Also, we can calculate the radius of a class as

$$r^\pm = \max_{y_i = \pm 1} \|\phi(x_i) - C^\pm\|. \quad (22)$$

It is visible in Fig. (1) that the data points lying in the intersection region of the two classes have the same membership values with respect to both classes.

2.5.2. Non-membership degree

The degree of non-membership for a data point is given by the ratio of the number of heterogeneous points and all points in its neighborhood. The non-membership function is written as:

$$\nu(x_i) = (1 - \mu(x_i))\rho(x_i), \quad (23)$$

where $\rho(x_i)$ can be calculated as

$$\rho(x_i) = \frac{|\{x_j | \|\phi(x_i) - \phi(x_j)\| \leq \gamma, y_j \neq y_i\}|}{|\{x_j | \|\phi(x_i) - \phi(x_j)\| \leq \gamma\}|}. \quad (24)$$

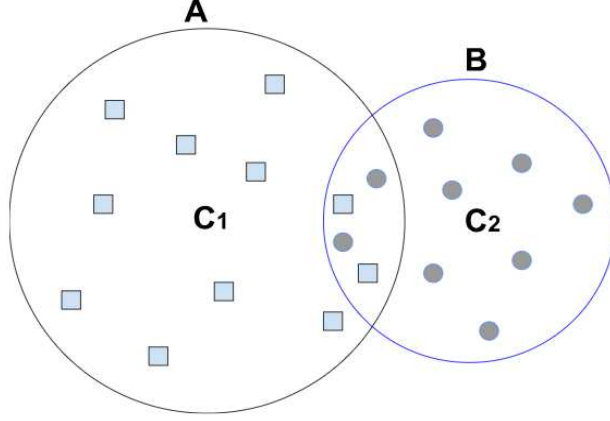


Figure 1: Similar degree of membership for the training samples.

In equation (24), $\gamma > 0$ is an adjustable parameter and $|A|$ represents the cardinality of A .

The training points are transformed into intuitionistic fuzzy numbers,

$$T = \left\{ \{x_1, y_1, \mu_1, \nu_1\}, \{x_2, y_2, \mu_2, \nu_2\}, \dots, \{x_l, y_l, \mu_l, \nu_l\} \right\}.$$

2.5.3. Score value

The score value for the training points is defined as:

$$k_i = \begin{cases} \mu_i, & \nu_i = 0, \\ 0, & \mu_i \leq \nu_i, \\ \frac{1-\nu_i}{2-\mu_i-\nu_i}, & \text{others.} \end{cases} \quad (25)$$

3. Proposed work

This section presents the proposed fuzzy membership assignment technique, and also discusses the linear and nonlinear formulations of the proposed algorithm.

3.1. Proposed intuitionistic fuzzy assignment

Since we are dealing with class imbalance, so we incorporate an imbalance ratio term in the existing score value (25). This makes the score more effective

in the class imbalance scenario.

The proposed fuzzy-based assignment to the slack factor is given by

$$S_i = \begin{cases} k_i, & x \in \text{majority class}, \\ IR \times k_i, & x \in \text{minority class}. \end{cases} \quad (26)$$

where IR is defined as:

$$IR = \frac{\text{Total samples of majority class}}{\text{Total samples of minority class}}. \quad (27)$$

In equation (27), the majority class is also referred as positive class, and minority class as negative class.

3.2. Proposed projection based fuzzy membership assignment (PFMA)

The existing fuzzy membership functions employed in various SVM variants exhibit certain limitations. One such drawback observed in the class center-based fuzzy membership is that these function assigns membership values solely based on the distance from the class center, disregarding whether the data point is closer to the proximal hyperplane of its own class or not. The proposed PFMA is based on the projection of the data point on the proximal hyperplane of its class. Nasiri et al. [14] proposed an energy-based least square twin support vector machine LSTSVM (ELS-TSVM) that reduces the influence of noise and outliers by incorporating an energy component for each hyperplane. We get our proximal hyperplanes by using ELS-TSVM, as mentioned in equations (12) and (13). We use SMW [25] formula to reduce computational cost and also incorporate $\delta > 0$ in both equations to avoid ill-conditioning and singularity issues of the matrices in (12) and (13). Then we calculate the projection of the data point on its class hyperplane and denote it by d_{hyp} .

$$d_{hyp}(x) = \frac{|w_i^T x + b_i|}{\|w_i\|}. \quad (28)$$

The proposed score value $h_i : X \rightarrow \mathbb{R}$ is defined as follows:

$$h(x_i) = \exp \left(- \frac{d_{hyp}(x_i) - \min_{x_i \in X} (d_{hyp}(x_i))}{\max_{x_i \in X} (d_{hyp}(x_i)) - \min_{x_i \in X} (d_{hyp}(x_i))} \right). \quad (29)$$

To deal with the imbalance issue in classification, we introduce an imbalance ratio term in the proposed fuzzy score value. The training points are transformed into fuzzy numbers,

$$T = \left\{ \{x_1, y_1, h_1\}, \{x_2, y_2, h_2\}, \dots, \{x_l, y_l, h_l\} \right\}.$$

Hence, our assigned fuzzy-based weight is $S_i : X \rightarrow \mathbb{R}$

$$S_i = \begin{cases} h_i, & x \in \text{majority class}, \\ IR \times h_i, & x \in \text{minority class}, \end{cases} \quad (30)$$

where IR is the same as defined in equation (27).

Proposition 1 : $h(x) = \exp\left(-\frac{d_{hyp}(x) - \min_{x \in X}(d_{hyp}(x))}{\max_{x \in X}(d_{hyp}(x)) - \min_{x \in X}(d_{hyp}(x))}\right)$ is a fuzzy function.

Proof :

$$\min_{x \in X}(d_{hyp}(x)) \leq d_{hyp}(x) \leq \max_{x \in X}(d_{hyp}(x)).$$

Therefore

$$0 \leq d_{hyp}(x) - \min_{x \in X}(d_{hyp}(x)) \leq \max_{x \in X}(d_{hyp}(x)) - \min_{x \in X}(d_{hyp}(x)).$$

$$\implies 0 \leq \frac{d_{hyp}(x) - \min_{x \in X}(d_{hyp}(x))}{\max_{x \in X}(d_{hyp}(x)) - \min_{x \in X}(d_{hyp}(x))} \leq 1,$$

or equivalently

$$0 \geq -\frac{d_{hyp}(x) - \min_{x \in X}(d_{hyp}(x))}{\max_{x \in X}(d_{hyp}(x)) - \min_{x \in X}(d_{hyp}(x))} \geq -1.$$

Since exponential is an increasing function, we have

$$e^{-1} \leq h_i(x) = \exp\left(-\frac{d_{hyp}(x) - \min_{x \in X}(d_{hyp}(x))}{\max_{x \in X}(d_{hyp}(x)) - \min_{x \in X}(d_{hyp}(x))}\right) \leq 1.$$

Hence, $h(x)$ takes values only in the interval $[e^{-1}, 1]$. Since $[e^{-1}, 1] \subseteq [0, 1]$, so the function $h(x)$ is a fuzzy membership function.

3.2.1. Properties of the proposed PFMA:

We discuss some properties of the proposed fuzzy membership function (29).

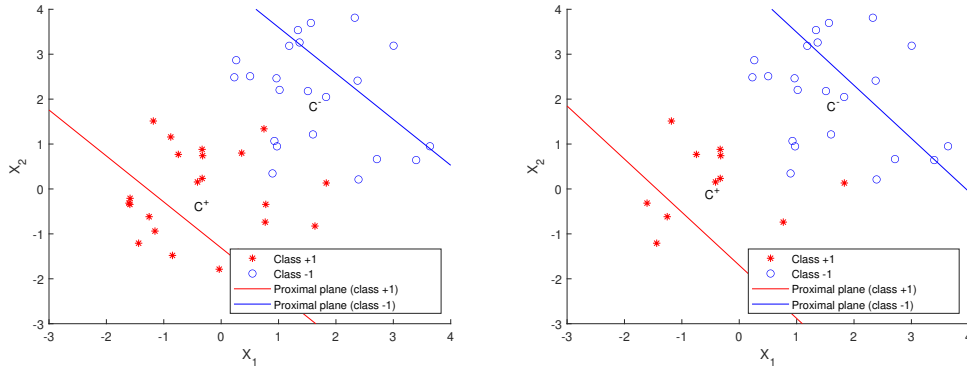
1. PFMA is based on proximal planes that are aligned to the distribution of data points, so the PFMA approach gives information about the data distribution for the fuzzy membership. This is in contrast to the centroid-based approach, where no information about data distribution is utilized for assigning the fuzzy membership.
2. The data point farthest from the proximal hyperplane corresponds to the minimum membership value.
3. PFMA takes values in the range $[e^{-1}, 1]$.
4. One can observe from Fig. (2) that the proximal planes are influenced by the data points of the other class in the proposed PFMA.

Some cases for the proposed PFMA approach are discussed below (see Fig. 3).

Case 1: Higher membership values are obtained for data points nearer to the proximal plane of their own class.

Case 2: Lower membership values are obtained for data points that are farther from their own proximal plane. The membership value decreases as the data point moves farther from its own proximal plane.

Case 3: Data points far from the proximal plane of its own class or close to the opposite class hyperplane get very low membership values.



(a) Plot of the proximal hyperplane of the binary artificial dataset. (b) Plot of the shifted proximal hyperplane of the binary reduced artificial dataset.

Figure 2: Plot showing the shift in both the proximal hyperplanes with change in only one class. The hyperplanes are generated using the proposed PFMA approach.

3.2.2. IFMA vs proposed PFMA

The IFMA approach assigns identical values to all the points having the same distance from the class centers. This technique awards the membership values based only on the distance from the centers. In contrast, the proposed PFMA distinguishes between the points based on their distance from the fixed proximal hyperplane. The points closest to the hyperplane get the highest membership values while the farthest point gets the least membership values. For instance, as shown in Fig. (4) points P and Q get nearly the same membership values in the IFMA approach but in the proposed PFMA approach point P has a higher membership value than point Q.

A noticeable difference between the two techniques is that it is possible in the new proposed PFMA for a point near the center to get a lower membership value. To illustrate, consider the points P, Q, and R in Fig. (4). In the IFMA approach, point R would get the higher membership among the three points P, Q, and R. On the other hand, in the proposed PFMA, point P would get the highest membership among the three, followed by R and then Q. This is due to the plane based membership calculation in the proposed PFMA, while in centroid-based membership functions the membership is based on distance from the class' centre (see Fig. 2).

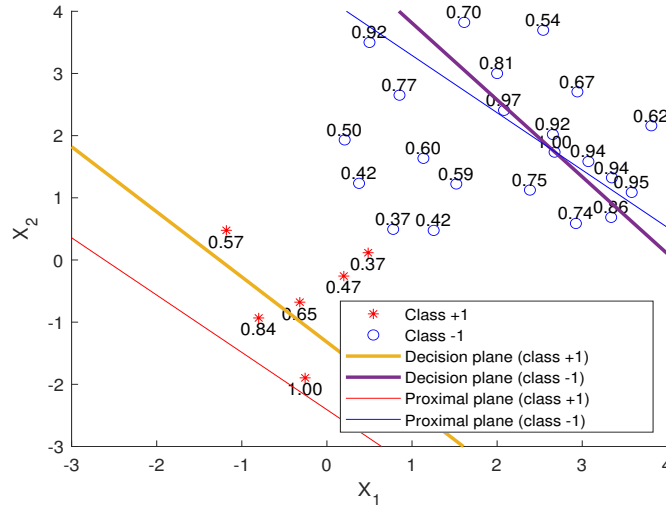


Figure 3: Plot showing membership values based on PFMA for an artificial dataset ($IR = 3.67$).

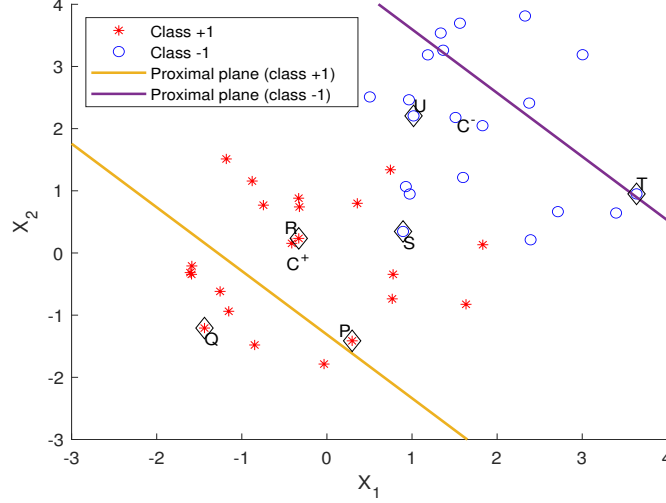


Figure 4: Fuzzy membership based on projection on proximal planes.

3.3. Proposed algorithms

By including regularisation terms into the framework of ELS-TSVM, we propose IF-RELSTSVMS and F-RELSTSVMS by using IFMA (equation (26)) and proposed PFMA (equation (29)), respectively. The linear and non-linear cases are discussed below:

3.3.1. Linear case

The optimization of the proposed algorithm is defined as:

$$\begin{aligned} \min_{w_1, b_1, \xi_2} \quad & \frac{1}{2} \|Aw_1 + e_1 b_1\|^2 + \frac{C_1}{2} (S_2 \xi_2)^T S_2 \xi_2 + \frac{1}{2} C_2 (\|w_1\|^2 + b_1^2) \\ \text{subject to} \quad & -(Bw_1 + e_2 b_1) + \xi_2 = E_2, \end{aligned} \quad (31)$$

and

$$\begin{aligned} \min_{w_2, b_2, \xi_1} \quad & \frac{1}{2} \|Bw_2 + e_2 b_2\|^2 + \frac{C_3}{2} (S_1 \xi_1)^T S_1 \xi_1 + \frac{1}{2} C_4 (\|w_2\|^2 + b_2^2) \\ \text{subject to} \quad & (Aw_2 + e_1 b_2) + \xi_1 = E_1, \end{aligned} \quad (32)$$

where S_i is fuzzy-based weights to penalties, C_1, C_2, C_3 and C_4 are regularization parameters and E_1, E_2 are energy parameters.

The Lagrangian for (31) is given by

$$L = \frac{1}{2} \|Aw_1 + e_1b_1\|^2 + C_1 \|S_2(Bw_1 + e_2b_1 + E_2)\|^2 + \frac{1}{2}C_2(\|w_1\|^2 + b_1^2). \quad (33)$$

Setting the gradient of (33) with respect to w_1 , b_1 and then equating it to zero gives:

$$\frac{\partial L}{\partial w_1} = A^T(Aw_1 + e_1b_1) + C_1(S_2B)^T S_2(Bw_1 + e_2b_1 + E_2) + C_2w_1 = 0, \quad (34)$$

$$\frac{\partial L}{\partial b_1} = e_1^T(Aw_1 + e_1b_1) + C_1(S_2B)^T S_2(Bw_1 + e_2b_1 + E_2) + C_2b_1 = 0. \quad (35)$$

Combining the above both equations, we get

$$\begin{bmatrix} A^T \\ e_1^T \end{bmatrix} \begin{bmatrix} A^T & e_1^T \end{bmatrix} \begin{bmatrix} w_1 \\ b_1 \end{bmatrix} + C_1 \begin{bmatrix} S_2B^T \\ S_2e_2^T \end{bmatrix} \left[\begin{bmatrix} S_2B & S_2e_2 \end{bmatrix} \begin{bmatrix} w_1 \\ b_1 \end{bmatrix} + S_2E_2 \right] + C_2 \begin{bmatrix} w_1 \\ b_1 \end{bmatrix} = 0. \quad (36)$$

Let $H_1 = \begin{bmatrix} A & e \end{bmatrix}$ and $G_2 = \begin{bmatrix} S_2B & S_2e \end{bmatrix}$, then (31) can be reformulated as:

$$\begin{bmatrix} w_1 \\ b_1 \end{bmatrix} = - \left(\frac{1}{C_1} H_1^T H_1 + G_2^T G_2 + \frac{C_2}{C_1} I \right)^{-1} G_2^T S_2 E_2. \quad (37)$$

Similarly, the solution for the other class is given by

$$\begin{bmatrix} w_2 \\ b_2 \end{bmatrix} = \left(\frac{1}{C_3} J_2^T J_2 + R_1^T R_1 + \frac{C_4}{C_3} I \right)^{-1} R_1^T S_1 E_1, \quad (38)$$

where $R_1 = \begin{bmatrix} S_1A & S_1e \end{bmatrix}$ and $J_2 = \begin{bmatrix} B & e \end{bmatrix}$. The linear IF-RELSTSVM training step is complete after acquiring two hyperplanes, (w_1, b_1) and (w_2, b_2) . We obtain the label of a new data point x using equation (14).

3.4. Non-linear case

In this section, we explore kernel-generated surfaces in place of planes and extend our results to nonlinear classifiers. Consider

$$K(x^T, C^T)w_{(1)} + b_{(1)} = 0 \text{ and } K(x^T, C^T)w_{(2)} + b_{(2)} = 0,$$

where $C^T = [A \ ; B]^T$, and K is the kernel function. The optimization problems for the non-linear case are written as:

$$\begin{aligned} \min_{w_1, b_1, \xi_2} \quad & \frac{1}{2} \| K(A, C^T)w_1 + e_1b_1 \|^2 + C_1(S_2\xi_2)^T S_2\xi_2 + \frac{1}{2}C_2(\| w_1 \|^2 + b_1^2) \\ \text{subject to} \quad & -(K(B, C^T)w_1 + e_2b_1) + \xi_2 = E_2, \end{aligned} \quad (39)$$

and

$$\begin{aligned} \min_{w_2, b_2, \xi_1} \quad & \frac{1}{2} \| K(B, C^T)w_2 + e_2b_2 \|^2 + C_3(S_1\xi_1)^T S_1\xi_1 + \frac{1}{2}C_4(\| w_2 \|^2 + b_2^2) \\ \text{subject to} \quad & (K(A, C^T)w_2 + e_1b_2) + \xi_1 = E_1, \end{aligned} \quad (40)$$

where the sizes of kernel matrices $K(A, C^T)$ and $K(B, C^T)$ are $p \times m$ and $q \times m$ respectively, $m = p + q$.

The Lagrangian for (39) is given by

$$L(w_1, b_1, \xi_2, \alpha, \beta) = \frac{1}{2} \| K(A, C^T)w_1 + e_1b_1 \|^2 + C_1(S_2\xi_2)^T S_2\xi_2 + \frac{1}{2}C_2(\| w_1 \|^2 + b_1^2). \quad (41)$$

Putting the values of ξ_2 in lagrangian (41), we get

$$\begin{aligned} L = & \frac{1}{2} \| K(A, C^T)w_1 + e_1b_1 \|^2 + \\ & C_1 \| S_2(K(B, C^T)w_1 + e_2b_1 + E_2) \|^2 + \frac{1}{2}C_2(\| w_1 \|^2 + b_1^2). \end{aligned} \quad (42)$$

Setting the gradient of (42) with respect to w_1 and b_1 to zero gives:

$$\frac{\partial L}{\partial w_1} = K(A, C^T)^T (K(A, C^T)w_1 + e_1b_1) + \quad (43)$$

$$C_1(S_2K(B, C^T))^T S_2(K(B, C^T)w_1 + e_2b_1 + E_2) + C_2w_1 = 0,$$

$$\frac{\partial L}{\partial b_1} = e_1^T (K(A, C^T)w_1 + e_1b_1) + \quad (44)$$

$$C_1(S_2K(B, C^T))^T S_2(K(B, C^T)w_1 + e_2b_1 + E_2) + C_2b_1 = 0.$$

Combining the above two equations, we get

$$\begin{aligned} & \begin{bmatrix} K(A, C^T)^T \\ e_1^T \end{bmatrix} \begin{bmatrix} K(A, C^T) & e_1 \end{bmatrix} \begin{bmatrix} w_1 \\ b_1 \end{bmatrix} + \\ & C_1 \begin{bmatrix} S_2 K(B, C^T)^T \\ S_2 e_2^T \end{bmatrix} \begin{bmatrix} [S_2 K(B, C^T) & S_2 e_2] \begin{bmatrix} w_1 \\ b_1 \end{bmatrix} S_2 E_2 \end{bmatrix} + C_2 \begin{bmatrix} w_1 \\ b_1 \end{bmatrix} = 0. \end{aligned} \quad (45)$$

Let $H_1 = [K(A, C^T) \ e_1]$ and $G_2 = [S_2 K(B, C^T) \ S_2 e_2]$, then (39) can be reformulated as

$$\begin{bmatrix} w_1 \\ b_1 \end{bmatrix} = - \left(\frac{1}{C_1} H_1^T H_1 + G_2^T G_2 + \frac{C_2}{C_1} I \right)^{-1} G_2^T S_2 E_2. \quad (46)$$

In a similar way, solution for other class is given by

$$\begin{bmatrix} w_2 \\ b_2 \end{bmatrix} = \left(\frac{1}{C_3} J_2^T J_2 + R_1^T R_1 + \frac{C_4}{C_3} I \right)^{-1} R_1^T S_1 E_1. \quad (47)$$

where $R_1 = [S_1 K(A, C^T) \ S_1 e_1]$ and $J_2 = [K(B, C^T) \ e_2]$.

Note: $(\frac{1}{C_3} J_2^T J_2 + R_1^T R_1 + \frac{C_4}{C_3} I)$ and $(\frac{1}{C_1} H_1^T H_1 + G_2^T G_2 + \frac{C_2}{C_1} I)$ are positive definite, which makes our model stable and robust than LSTSVM and ELS-TSVM. Moreover, the solution of nonlinear F-RELSTSVM and IF-RELSTSVM requires the two matrix inverse of size $(m+1) \times (m+1)$. As a result, the SMW formula is employed to approximate and decrease the above equation's computation costs.

Case 1: $p < q$

$$\begin{bmatrix} w_1 \\ b_1 \end{bmatrix} = - \left(Y - Y H_1^t (C_1 I + H_1 Y H_1^t)^{-1} H_1 Y \right) V^t E_2, \quad (48)$$

where $Y = \frac{C_1}{C_2} \left(I - G_2^t \left(\frac{C_2}{C_1} I + G_2 G_2^t \right)^{-1} G_2 \right)$.

$$\begin{bmatrix} w_2 \\ b_2 \end{bmatrix} = C_2 \left(Y_1 - Y_1 J_2^t \left(\frac{I}{C_2} + J_2 Y_1 J_2^t \right)^{-1} J_2 Y_1 \right) J_2^t E_1, \quad (49)$$

where $Y_1 = \frac{C_3}{C_4} \left(I - R_1^t \left(\frac{C_4}{C_3} I + R_1 R_1^t \right)^{-1} R_1 \right)$.

Case 2: $q < p$

$$\begin{bmatrix} w_1 \\ b_1 \end{bmatrix} = -C_1 \left(Z - Z G_2^t \left(\frac{I_2}{C_1} + G_2 Z^t G_2 \right)^{-1} G_2 Z \right) G_2^t E_2, \quad (50)$$

where $Z = \frac{C_1}{C_2} \left(I - H_1^t \left(\frac{C_2}{C_1} I + H_1 H_1^t \right)^{-1} H_1 \right)$.

$$\begin{bmatrix} w_2 \\ b_2 \end{bmatrix} = \left(Z_1 - Z_1 R_1^t (C_2 I + R_1 Z_1 R_1^t)^{-1} R_1 Z_1 \right) R_1^t E_1, \quad (51)$$

where $Z_1 = \frac{C_3}{C_4} \left(I - J_2^t \left(\frac{C_4}{C_3} I + J_2 J_2^t \right)^{-1} J_2 \right)$.

The label of an unknown data point x is assigned to class ($i = +1, -1$) based on the decision function below.

$$\text{Class label}(x) = \begin{cases} +1, & \frac{|K(x_i, C^T)w_1 + b_1|}{|K(x_i, C^T)w_2 + b_2|} \leq 1, \\ -1, & \frac{|K(x_i, C^T)w_1 + b_1|}{|K(x_i, C^T)w_2 + b_2|} > 1, \end{cases} \quad (52)$$

Proposition 2 : For any given C_1 and $C_2 > 0$, $\left\{ \frac{1}{C_1} H_1^T H_1 + \frac{C_2}{C_1} I + G_2^T G_2 \right\}$ is a invertible matrix.

Proof : Let x be a non-zero column vector of $(m+1) \times 1$ order. Now,

$$\begin{aligned} x^T (H_1^T H_1) x &= (H_1 x)^T (H_1 x), \\ &= \|H_1 x\|^2 \geq 0. \end{aligned}$$

Since for any $C_1 > 0$, $\frac{1}{C_1} H_1^T H_1$ and $G_2^T G_2$ are positive semi-definite matrices, so $\left\{ \frac{1}{C_1} H_1^T H_1 + G_2^T G_2 \right\}$ is a positive semi-definite matrix. Now, as I (identity) is a positive definite matrix, therefore, for all C_1 and $C_2 > 0$, $\left\{ \frac{1}{C_1} H_1^T H_1 + \frac{C_2}{C_1} I + G_2^T G_2 \right\}$ is a positive definite matrix, and hence invertible.

3.5. Computational complexity

Here, we describe the computation complexity of the proposed algorithm. The proposed algorithm maintains the same size for the invertible matrices as in LSTSVM, thereby avoiding additional computational overhead when

solving the optimization problem. In the LSTSVM formulation, two matrix inverses are calculated of size $(m+1) \times (m+1)$, where m represents the sum of the number of data points in the positive and negative classes (denoted as p and q , respectively). To streamline the computation of inverses, the Sherman-Morrison-Woodbury (SMW) formula [25] is employed. This formula allows us to solve three inverses of smaller sizes.

The computation required for the proposed algorithms involves the fuzzy membership degree calculation. However, our IFMA has a time complexity of $O(m)$, as they calculate fuzzy membership for all data points using measures like distance from the centroid.

The proposed PFMA involves matrix inverse, in the case where $p < q$, the nonlinear PFMA requires two matrix inverses of size $(p \times p)$ and one matrix inverse of size $(q \times q)$. Conversely, when $q < p$, the algorithm necessitates two matrix inverses of size $(q \times q)$ and one matrix inverse of size $(p \times p)$.

4. Numerical experiments

In this section, we perform numerical experiments to compare the proposed F-RELSTSVM and IF-RELSTSVM methods with the baseline models and also perform statistical analysis to demonstrate the significance of the proposed models.

4.1. Parameter selection

We demonstrate the effectiveness of the proposed fuzzy membership assignment by comparing the proposed F-RELSTSVM and IF-RELSTSVM with other baseline algorithms such as LSTSVM [12], ELS-TSVM [14], RELS-TSVM [15], and IFLSTSVM [17] on different synthetic and real world imbalanced datasets. To determine the best parameters, a five-fold cross-validation technique, along with grid search, is employed for all the algorithms. The Gaussian kernel is given by $K(x_i, x_k) = \exp\left(-\frac{\|x_i - x_k\|^2}{2\sigma}\right)$, where $x_i, x_k \in \mathbb{R}^m$ are the input vectors and σ is the kernel parameter. To compare the algorithms, the AUC [22] is calculated as,

$$\text{AUC} = \frac{1 + T_P - F_P}{2}.$$

Here, T_P represents the true positive rate and F_P represents the false positive rate. The value of Gaussian kernel parameter σ for all the algorithms is selected from the set $\{2^i | i = -5, -4, \dots, 5\}$. The value of the parameters $C_i, i =$

$\{1, 2, 3, 4\}$ and $E_i, i = \{1, 2\}$ are chosen from the sets $\{10^i | i = -5, -4, \dots, 5\}$ and $\{0.6, 0.7, 0.8, 0.9, 1\}$ respectively for both linear and nonlinear kernels. In order to reduce the training cost, we set $C_1 = C_2$ for LSTSVM, ELS-TSVM, and $C_1 = C_2, C_3 = C_4$ for IFLSTSVM, RELS-TSVM, F-RELSTSVM, and IF-RELSTSVM. In this study, the AUC values for all the algorithms are expressed as percentages.

4.2. Real world datasets

To assess the performance of the proposed IF-RELSTSVM and F-RELSTSVM algorithms, we compare proposed algorithms to LSTSVM, ELS-TSVM, IFLSTSVM, and RELS-TSVM on 29 datasets from the KEEL repository [26, 27]. We can observe from Table (1) and (3) that for linear kernel, the proposed IF-RELSTSVM and F-RELSTSVM outperform all other baseline algorithms with higher average AUC, *i.e.* 81.94 and 82.21, respectively. The average ranks of all the algorithms using AUC were calculated and presented in Table (2).

4.3. Statistical analysis on real world datasets

In this sub-section, we perform a statistical analysis of the compared models to demonstrate the significance of the proposed IF-RELSTSVM and F-RELSTSVM models. The statistical tests are performed using the Friedman and Nemenyi post-hoc test [28].

Friedman test: We statistically assess the models using the Friedman test. Under the null hypothesis, we assume that all the algorithms are similar, *i.e.*, the average rank of all algorithms is equal. The Friedman test follows the chi-squared distribution (χ_F^2) with $(k - 1)$ degrees of freedom (k is the number of models), and N datasets. The chi-squared (χ_F^2) distribution is calculated using Table (2) as,

$$\chi_F^2 = \frac{12N}{k(k+1)} \left[\sum_{j=1}^k R_j^2 - \frac{k(k+1)^2}{4} \right], \quad (53)$$

$$\chi_F^2 = \frac{12 \times 29}{6(6+1)} \left[4.47^2 + 3.57^2 + 3.45^2 + 3.47^2 + 3.05^2 + 3^2 - \frac{6(7)^2}{4} \right] \quad (54)$$

$$= 11.52,$$

$$F_F = \frac{(N-1)\chi_F^2}{N(k-1) - \chi_F^2} = \frac{(29-1) \times 11.52}{29(6-1) - 11.52} = 2.42. \quad (55)$$

where the F_F value is as per the F -distribution with degrees of freedom $(k-1)$ and $(k-1)(N-1)$, i.e., $(5, 140)$, as we are considering the inclusion of 6 algorithms and 29 datasets with linear kernel. For a significance level of $\alpha = 0.05$, the critical value of $F(5, 140)$ amounts to 2.28. Since the obtained F_F value surpasses the critical value, we reject the null hypothesis.

Also, to examine the significant difference between the algorithms we employ the Nemenyi post-hoc test.

Nemenyi post-hoc test: To perform pairwise comparisons, we utilize the Nemenyi post-hoc test. At a significance level of $p = 0.10$, CD is calculated to be 1.27.

$$CD = 2.589 \times \sqrt{\frac{6 \times 7}{6 \times 29}} = 1.27.$$

As evident from Fig. (5), the proposed F-RELSTSVM algorithm has a significant difference (1.46) with LSTSVM, while no significant difference with the other baseline algorithms for the linear kernel. Also, it can be seen that the proposed IF-RELSTSVM is the second best in terms of average rank among these algorithms.

To further compare the performance of six algorithms, we statistically analyze the AUC using a Gaussian kernel. The average ranks of all the algorithms based on their AUC are computed and presented in Table 4. The Friedman statistic will be employed under the assumption of the null hypothesis.

$$\chi_F^2 = \frac{12 \times 29}{6(6+1)} \left[3.69^2 + 4.10^2 + 4.09^2 + 3.39^2 + 3.39^2 + 2.33^2 - \frac{6(7)^2}{4} \right], \quad (56)$$

$$= 17.72$$

$$F_F = \frac{(N-1)\chi_F^2}{N(k-1) - \chi_F^2} = \frac{(29-1) \times 17.72}{29(6-1) - 17.72} = 3.90, \quad (57)$$

Again, considering the inclusion of 6 algorithms and 29 datasets, the computed F_F value adheres to the F -distribution with degrees of freedom $(k-1)$

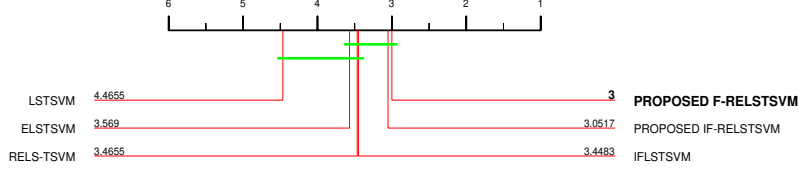


Figure 5: Critical difference diagram with linear kernel on real world datasets.

and $(k - 1)(N - 1) = (5, 140)$. For a significance level of $\alpha = 0.05$, the critical value for $F(5, 140)$ is 2.28, and the CD is 1.27. The obtained F_F value surpasses the critical value, we can reject the null hypothesis. Since the difference between the rank of proposed F-RELSTSVM to LSTSVM, ELS-TSVM, and IFLSTSVM is greater than 1.27, $(3.69 - 2.33) = 1.36$, $(4.10 - 2.33) = 1.77$, $(4.09 - 2.33) = 1.76$, respectively, hence the proposed F-RELSTSVM has a significant difference from the other baseline algorithms. Also, the proposed IF-RELSTSVM has lower average rank than LSTSVM, IFLSTSVM, and ELSTSVM algorithms. Similar to the linear case, F-RELSTSVM and IF-RELSTSVM have lower ranks than all the other algorithms, as shown in Fig. (6).

4.4. Noise and synthetic datasets

To assess the effectiveness of the proposed F-RELSTSVM and IF-RELSTSVM methods, we conducted experiments using synthetic datasets. Specifically, we utilized noisy synthetic datasets in our analysis. These datasets are obtained from the KEEL imbalanced datasets repository [26, 27]. The datasets consist of two classes with data points randomly and uniformly distributed in a two-dimensional space (both attributes being real-valued). The noisy datasets used in our experiments were identified with different disturbance ratios of 30%, 50%, and 60% [27]. From Table 5, it is evident that the proposed approach achieves the lowest rank with the highest average AUC with

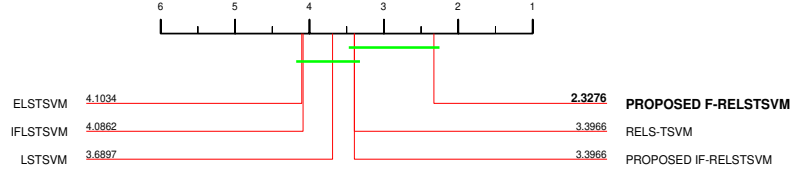


Figure 6: Critical difference diagram with Gaussian kernel on real world datasets.

Table 1 Performance comparison on real world datasets with linear kernel.

DATASETS	LSTVM [12]	ELS-TSVM [14]	IFLSTVM [17]	RELS-TSVM [15]	Proposed IF-RELSTVM	Proposed F-RELSTVM
	AUC(%), Time(s)	AUC(%), Time(s)	AUC(%), Time(s)	AUC(%), Time(s)	AUC(%), Time(s)	AUC(%), Time(s)
Abalone9-18	84.82, 0.00699	83.16, 0.00221	84.82, 0.03212	79.31, 0.00722	84.58, 0.03643	85.31 , 0.02254
Brwiconsin	96.2, 0.00432	92.72, 0.00039	96.25, 0.02154	92.72, 0.00251	94.67, 0.0245	97.43 , 0.0139
Bupa or liver-disorders	62.64, 0.00152	63.36, 0.00039	66.03, 0.00549	67.43, 0.0013	69.99 , 0.00884	60.02, 0.00511
Crossplane150	100 , 0.00243	100 , 0.00009	100 , 0.0028	100 , 0.00025	100 , 0.00533	100 , 0.00627
Ecoli_0_1_4_6-vs-5	93.21, 0.00104	85.19, 0.0001	95.06, 0.00303	85.19, 0.00089	96.91 , 0.00524	96.3, 0.00201
Ecoli_0_1_4_7-vs-5_6	74.44, 0.00072	80, 0.00009	85.56, 0.00417	80, 0.00105	86.11, 0.00414	86.67 , 0.00218
Ecoli_0_1-vs-2_3_5	59.09, 0.0005	86.07 , 0.00014	84.75, 0.00252	81.82, 0.00051	84.75, 0.00274	86.07 , 0.00157
Ecoli_0_1-vs-5	87.5, 0.00049	86.72, 0.00007	92.97, 0.003	93.75 , 0.00046	93.75 , 0.00293	82.03, 0.00142
Ecoli_0_2_6_7-vs-3_5	64.29, 0.00075	68.93, 0.00008	71.07 , 0.00233	68.93, 0.00117	69.76, 0.00293	68.93, 0.00152
Ecoli_0_3_4_7-vs-5_6	84.85, 0.0007	84.85, 0.00007	84.85, 0.00293	80.3, 0.00074	85.61 , 0.00276	85.61 , 0.00159
Ecoli01vs5	94.44, 0.00071	99.21 , 0.00007	99.21 , 0.00319	99.21 , 0.00068	98.41, 0.00343	98.41, 0.00139
Ecoli4	97.31 , 0.00068	78.57, 0.00007	97.31 , 0.00442	94.09, 0.00107	97.31 , 0.00768	96.77, 0.00212
Glass_0_1_4_6-vs-2	41.23, 0.00041	77.85 , 0.00007	47.59, 0.0039	77.85 , 0.00067	42.11, 0.00288	76.97, 0.00133
Glass_0_1_6-vs-5	92.45, 0.0006	98.11, 0.00007	100 , 0.00315	100 , 0.00055	96.23, 0.00331	89.62, 0.00152
Glass_0_6-vs-5	90, 0.00024	95, 0.00007	95, 0.00209	95, 0.00041	100 , 0.00164	95, 0.00069
Glass2	58.05, 0.00066	81.32 , 0.00008	69.83, 0.0025	81.32 , 0.00071	77.01, 0.00338	74.71, 0.00143
Glass4	55.36, 0.00065	83.93 , 0.00007	58.93, 0.00264	77.68, 0.00059	83.93 , 0.0044	65.18, 0.00154
Haber	65.15, 0.00088	58.66, 0.00006	73.82 , 0.00241	68.8, 0.00059	67.33, 0.004	73.08, 0.00191
Monk1	50 , 0.00189	50 , 0.00012	44.73, 0.00573	47.25, 0.00107	48.38, 0.00843	50 , 0.0038
Monk2	50, 0.00191	63.89, 0.00018	50, 0.00672	64.68, 0.00115	66.01, 0.009	73.28 , 0.00429
New-thyroid1	98.21, 0.00043	98.21, 0.00006	98.21, 0.00178	99.11 , 0.00044	99.11 , 0.0026	99.11 , 0.00135
Shuttle_6-vs-2_3	100 , 0.00057	100 , 0.00011	100 , 0.00218	100 , 0.00053	99.25, 0.00259	99.25, 0.0014
Shuttle_c0-vs-c4	100 , 0.02903	100 , 0.00027	100 , 0.05638	100 , 0.0308	100 , 0.10022	100 , 0.07682
Transfusion	57.48, 0.0041	64.15 , 0.00016	55.54, 0.00868	62.67, 0.00291	60.56, 0.01304	59.04, 0.00894
Vehicle 1	77.34, 0.00465	79.44, 0.00024	77.6, 0.01558	79.7, 0.00362	74.14, 0.02129	80.76 , 0.01202
Yeast_0_2_5_6-vs-3_7_8_9	71.86, 0.00671	76.3, 0.00024	75.19, 0.02493	74.82, 0.00671	78.16 , 0.03683	76.49, 0.02153
Yeast_0_3_5_9-vs-7_8	63.19, 0.00133	63.94 , 0.00016	62.08, 0.00739	63.94 , 0.00134	62.82, 0.0094	62.82, 0.00422
Yeast1vs7	68.33, 0.00162	68.15 , 0.00018	75.87, 0.01066	68.15, 0.00154	66.16, 0.0082	71.68, 0.00381
Yeast3	92.66, 0.01549	88.05, 0.00026	92.54, 0.0497	89.49, 0.01651	93.24, 0.06955	93.49 , 0.04338
Average AUC(%), Average time(s)	76.9, 0.00317	81.23, 0.00021	80.51, 0.01014	81.83, 0.00303	81.94 , 0.01406	82.21 , 0.00868

Table 2 Comparison on ranks based on AUC for real world datasets with linear kernel.

DATASETS	LSTSVM [12]	ELS-TSVM [14]	IFLSTSVM [17]	RELS-TSVM [15]	Proposed IF-RELSTSVM	Proposed F-RELSTSVM
Abalone9-18	2.5	5	2.5	6	4	1
Brwiscosin	3	5.5	2	5.5	4	1
Bupa or liver-disorders	5	4	3	2	1	6
Crossplane150	3.5	3.5	3.5	3.5	3.5	3.5
Ecoli_0_1_4_6-vs-5	4	5.5	3	5.5	1	2
Ecoli_0_1_4_7-vs-5_6	6	4.5	3	4.5	2	1
Ecoli_0_1-vs-2_3_5	6	1.5	3.5	5	3.5	1.5
Ecoli_0_1-vs-5	4	5	3	1.5	1.5	6
Ecoli_0_2_6_7-vs-3_5	6	4	1	4	2	4
Ecoli_0_3_4_7-vs-5_6	4	4	4	6	1.5	1.5
Ecoli01vs5	6	2	2	2	4.5	4.5
Ecoli4	2	6	2	5	2	4
Glass_0_1_4_6-vs-2	6	1.5	4	1.5	5	3
Glass_0_1_6-vs-5	5	3	1.5	1.5	4	6
Glass_0_6-vs-5	6	3.5	3.5	3.5	1	3.5
Glass2	6	1.5	5	1.5	3	4
Glass4	6	1.5	5	3	1.5	4
Haber	5	6	1	3	4	2
Monk1	2	2	6	5	4	2
Monk2	5.5	4	5.5	3	2	1
New-thyroid1	5	5	5	2	2	2
Shuttle_6-vs-2_3	2.5	2.5	2.5	2.5	5.5	5.5
Shuttle_c0-vs-c4	3.5	3.5	3.5	3.5	3.5	3.5
Transfusion	5	1	6	2	3	4
Vehicle 1	5	3	4	2	6	1
Yeast_0_2_5_6-vs-3_7_8_9	6	3	4	5	1	2
Yeast_0_3_5_9-vs-7_8	3	1.5	6	1.5	4.5	4.5
Yeast1vs7	3	4.5	1	4.5	6	2
Yeast3	3	6	4	5	2	1
Average rank	4.47	3.57	3.45	3.47	3.05	3

Table 3 Performance comparison on real world datasets with Gaussian kernel.

DATASETS	LTSVM [12]	ELS-TSVM [14]	IFLTSVM [17]	RELS-TSVM [15]	Proposed IF-RELSTSV	Proposed F-RELSTSV
	AUC(%), Time(s)	AUC(%), Time(s)	AUC(%), Time(s)	AUC(%), Time(s)	AUC(%), Time(s)	AUC(%), Time(s)
Abalone9-18	80.49, 0.04575	82.19, 0.11635	79.56, 0.11343	82.43 , 0.05702	73.53, 0.08418	82.19, 0.14283
Brwiconsin	95.94, 0.0281	97.38, 0.01777	97.43, 0.05074	97.79 , 0.05163	97.43, 0.04809	97.43, 0.05744
Bupa or liver-disorders	57.39, 0.00433	55.61, 0.00337	60.46, 0.01235	68.99 , 0.00598	61.52, 0.01678	62.58, 0.01725
Crossplane150	100 , 0.00467	100 , 0.00133	98.21, 0.0044	100 , 0.00131	100 , 0.00647	100 , 0.01177
Ecoli_0_1_4_6-vs-5	99.38 , 0.00204	99.38 , 0.00232	98.15, 0.00602	98.15, 0.00417	98.77, 0.00599	98.77, 0.00707
Ecoli_0_1_4_7-vs-5_6	81.67, 0.0057	71.67, 0.00293	81.11, 0.00802	71.67, 0.00596	76.11, 0.00825	86.11 , 0.00883
Ecoli_0_1-vs-2_3_5	81.82, 0.00322	77.27, 0.00179	86.36, 0.00582	90.10 , 0.00315	81.82, 0.00498	85.56, 0.00517
Ecoli_0_1-vs-5	81.25, 0.00176	81.25, 0.00192	87.5, 0.00455	83.59, 0.00291	87.5, 0.00578	91.41 , 0.00546
Ecoli_0_2_6_7-vs-3_5	70.6, 0.00132	71.43, 0.00171	80.71 , 0.00436	71.43, 0.00272	79.05, 0.00526	80.71 , 0.00455
Ecoli_0_3_4_7-vs-5_6	87.12, 0.00199	80.3, 0.00203	83.33, 0.00407	86.36, 0.00312	88.64, 0.00591	91.67 , 0.00482
Ecoli01vs5	98.41, 0.00189	99.21, 0.00167	97.62, 0.00565	100 , 0.00296	98.41, 0.00714	98.41, 0.00501
Ecoli4	96.24, 0.00267	85.71, 0.00296	92.86, 0.00845	95.7, 0.00612	97.85 , 0.01172	96.77, 0.00936
Glass_0_1_4_6-vs-2	44.96, 0.00156	44.96, 0.00168	57.46, 0.00477	62.72, 0.00254	37.72, 0.00986	67.11 , 0.00367
Glass_0_1_6-vs-5	73.11, 0.00121	99.06 , 0.00142	73.11, 0.00479	99.06 , 0.00216	97.17, 0.00484	97.17, 0.00326
Glass_0_6-vs-5	100 , 0.00122	100 , 0.00059	100 , 0.003	100 , 0.00094	100 , 0.00293	100 , 0.00185
Glass2	61.49, 0.00155	48.56, 0.00155	58.33, 0.00521	51.44, 0.00194	65.52 , 0.00586	54.02, 0.00422
Glass4	95.54 , 0.00141	77.68, 0.00164	81.25, 0.00628	84.82, 0.00198	82.14, 0.00584	91.07, 0.00381
Haber	67.17, 0.00274	69.47 , 0.00222	62.28, 0.00779	69.37, 0.0042	68, 0.0083	69.41, 0.00667
Monk1	46.62, 0.0086	50, 0.01137	40.37, 0.02167	50.25, 0.01595	47.66, 0.02907	57.25 , 0.02955
Monk2	79.37 , 0.02808	77.38, 0.02313	71.69, 0.02916	77.38, 0.03997	71.69, 0.04417	77.78, 0.07508
New-thyroid1	93.75 , 0.00154	85.71, 0.00152	87.5, 0.00521	92.86, 0.00265	81.25, 0.00495	93.75 , 0.00414
Shuttle_6-vs-2_3	50, 0.00143	50, 0.00138	98.51 , 0.00433	98.51 , 0.0029	97.76, 0.00497	98.51 , 0.00443
Shuttle_c0-vs-c4	99.9 , 0.20172	99.8, 0.16058	99.9 , 0.31575	99.8, 0.4391	99.9 , 0.4381	99.9 , 0.52959
Transfusion	56.85, 0.02267	55.53, 0.05365	57.9, 0.07529	54.33, 0.23136	60.21 , 0.04921	55.19, 0.04601
Vehicle 1	66.47, 0.02946	64.61, 0.02369	67.24, 0.04773	76.28, 0.04773	67.51, 0.06212	76.55 , 0.07874
Yeast_0_2_5_6-vs-3_7_8_9	76.67 , 0.04745	76.67 , 0.03281	72.79, 0.07591	71.86, 0.0727	71.86, 0.12351	73.71, 0.10853
Yeast_0_3_5_9-vs-7_8	61.71, 0.00651	63.56, 0.0048	63.19, 0.01574	60.81, 0.01086	65.42 , 0.01965	63.94, 0.01868
Yeast1vs7	61.83, 0.00536	73.09 , 0.00477	57.29, 0.01699	65.98, 0.00859	63.6, 0.01888	67.17, 0.01519
Yeast3	94.47, 0.12713	91.95, 0.07478	93.65, 0.16045	91.67, 0.23954	96.07 , 0.24887	95.95, 0.32764
Average AUC(%), Average time(s)	77.94, 0.02045	76.88, 0.01923	78.82, 0.03545	81.15 , 0.04387	79.8, 0.04454	83.11 , 0.05313

Table 4 Comparison on ranks based on AUC for real world datasets with Gaussian kernel.

DATASETS	LSTSVM [12]	ELS-TSVM [14]	IFLSTSVM [17]	RELS-TSVM [15]	Proposed IF-RELSTSVM	Proposed F-RELSTSVM
Abalone9-18	4	2.5	5	1	6	2.5
Brwiconsin	6	5	3	1	3	3
Bupa or liver-disorders	5	6	4	1	3	2
Crossplane150	3	3	6	3	3	3
Ecoli_0_1_4_6-vs-5	1.5	1.5	5.5	5.5	3.5	3.5
Ecoli_0_1_4_7-vs-5_6	2	5.5	3	5.5	4	1
Ecoli_0_1-vs-2_3_5	4.5	6	2	1	4.5	3
Ecoli_0_1-vs-5	5.5	5.5	2.5	4	2.5	1
Ecoli_0_2_6_7-vs-3_5	6	4.5	1.5	4.5	3	1.5
Ecoli_0_3_4_7-vs-5_6	3	6	5	4	2	1
Ecoli01vs5	4	2	6	1	4	4
Ecoli4	3	6	5	4	1	2
Glass_0_1_4_6-vs-2	4.5	4.5	3	2	6	1
Glass_0_1_6-vs-5	5.5	1.5	5.5	1.5	3.5	3.5
Glass_0_6-vs-5	3.5	3.5	3.5	3.5	3.5	3.5
Glass2	2	6	3	5	1	4
Glass4	1	6	5	3	4	2
Haber	5	1	6	3	4	2
Monk1	5	3	6	2	4	1
Monk2	1	3.5	5.5	3.5	5.5	2
New-thyroid1	1.5	5	4	3	6	1.5
Shuttle_6-vs-2_3	5.5	5.5	2	2	4	2
Shuttle_c0-vs-c4	2.5	5.5	2.5	5.5	2.5	2.5
Transfusion	3	4	2	6	1	5
Vehicle 1	5	6	4	2	3	1
Yeast_0_2_5_6-vs-3_7_8_9	1.5	1.5	4	6	5	3
Yeast_0_3_5_9-vs-7_8	5	3	4	6	1	2
Yeast1vs7	5	1	6	3	4	2
Yeast3	3	5	4	6	1	2
Average rank	3.69	4.10	4.09	3.39	3.39	2.33

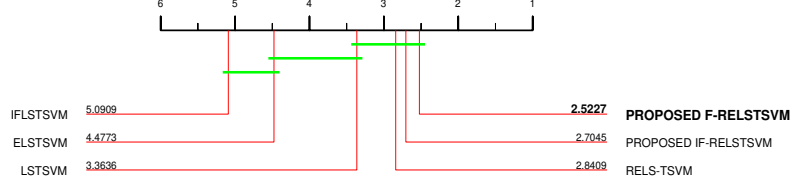


Figure 7: Critical difference diagram with Gaussian kernel on noise and synthetic datasets

linear kernel in F-RELSTSVM. We also conducted experiments on the cross-plane (XOR) dataset [29], which involved generating datasets with varying sample sizes and imbalance ratios. The datasets were created using randomized values in the equation of a line, $y = mx + b$. For the negative class, we selected the slope parameters $m = 0.7$ and intercept $b = 0.1$. Conversely, for the positive class, we chose parameter values as $m = -0.6$ and $b = 1$.

4.4.1. Statistical analysis on synthetic datasets

To assess the statistical significance of the proposed F-RELSTSVM and IF-RELSTSVM, we employ the Friedman test along with the corresponding post-hoc test. This analysis is performed on 22 noisy and synthetic binary class datasets with Gaussian kernel. Under the null hypothesis, we assume that all algorithms perform equivalently. The Friedman statistic is computed based on the ranks of the AUC values presented in Table (8).

$$\chi_F^2 = \frac{12 \times 22}{6(6+1)} \left[3.36^2 + 4.48^2 + 5.09^2 + 2.84^2 + 2.7^2 + 2.52^2 - \frac{6(7)^2}{4} \right] \quad (58)$$

$$= 34.38,$$

$$F_F = \frac{(N-1)\chi_F^2}{N(k-1) - \chi_F^2} = \frac{(22-1) \times 34.38}{22(6-1) - 34.38} = 9.54. \quad (59)$$

The value F_F is distributed according to the F -distribution with degrees of

Table 5 Performance comparison on synthetic datasets with linear kernel.

DATASETS	LTSVM [12]	ELS-TSVM [14]	IFLTSVM [17]	RELS-TSVM [15]	Proposed IF-RELSTSV	Proposed F-RELSTSV
	AUC(%), Time(s)	AUC(%), Time(s)	AUC(%), Time(s)	AUC(%), Time(s)	AUC(%), Time(s)	AUC(%), Time(s)
03subcl5-600-5-0-BI	50, 0.00386	50, 0.00123	59.12, 0.01982	64.19, 0.00378	59.71, 0.02455	64.44 , 0.01371
03subcl5-600-5-30-BI	58.57, 0.00266	59.92, 0.00032	51.35, 0.01596	63.01 , 0.00277	61.66, 0.01555	58.61, 0.01092
03subcl5-600-5-50-BI	57.77, 0.0028	53.38, 0.00036	50, 0.0078	58.53, 0.00269	61.87 , 0.0142	60.22, 0.00941
03subcl5-600-5-70-BI	50, 0.00507	50, 0.00159	49.03, 0.02128	55.74, 0.00642	56, 0.02325	63.85 , 0.01488
03subcl5-800-7-0-BI	55.99, 0.00657	59.41, 0.00015	55.3, 0.01383	68.66, 0.00913	69.02 , 0.01652	59.69, 0.01489
03subcl5-800-7-30-BI	47.32, 0.00671	45.11, 0.00017	51.08, 0.0145	60.3 , 0.00497	58.69, 0.01904	58.36, 0.01587
03subcl5-800-7-50-BI	55.2, 0.00497	55.49, 0.0002	47.92, 0.01476	59.15 , 0.00512	58.69, 0.01724	57.66, 0.01893
03subcl5-800-7-60-BI	53.23, 0.00528	52.3, 0.00019	53.69, 0.01017	59.91, 0.005	66.95 , 0.02366	56.02, 0.01495
03subcl5-800-7-70-BI	48.08, 0.00501	50.25, 0.00019	50, 0.01387	54.11 , 0.00527	52.99, 0.01699	53.09, 0.01518
04clover5z-600-5-30-BI	63.3, 0.00246	59.12, 0.00018	65.12, 0.00625	58.23, 0.00191	67.69 , 0.00864	61.95, 0.00473
04clover5z-600-5-50-BI	51.69, 0.00298	50, 0.00015	58.45, 0.00636	54.05, 0.00233	60.43 , 0.0091	53, 0.00502
04clover5z-600-5-60-BI	53.38, 0.00218	50, 0.00017	51.01, 0.00657	50, 0.00208	47, 0.01381	64.57 , 0.0049
04clover5z-800-7-30-BI	50, 0.00501	51.96, 0.00017	58.98, 0.01124	51.96, 0.00494	67.76 , 0.03004	54.8, 0.01835
04clover5z-800-7-50-BI	57.76, 0.00487	55.66, 0.00017	62.33 , 0.0104	57.5, 0.00508	61.48, 0.02089	56.61, 0.01226
04clover5z-800-7-60-BI	59.91, 0.0054	55.76, 0.00013	63.71 , 0.01173	50, 0.00513	45.17, 0.02329	40.13, 0.0148
04clover5z-800-7-70-BI	50, 0.00526	50, 0.00018	67.83 , 0.01101	50, 0.00553	58.59, 0.02075	55.85, 0.02297
Paw02a-600-5-0-BI	50, 0.00217	50, 0.00015	50, 0.00813	58.78, 0.00211	61.87 , 0.01249	44.26, 0.00886
Paw02a-600-5-30-BI	58.45, 0.00226	57.77, 0.00016	63.34 , 0.00659	56.33, 0.00216	54.48, 0.01195	62.25, 0.00962
Paw02a-800-7-0-BI	51.15, 0.00483	61.42, 0.00015	50, 0.01007	61.88, 0.00518	57.66, 0.02142	68.03 , 0.01132
Paw02a-800-7-30-BI	57.37, 0.00467	58.36, 0.00015	61.98 , 0.00988	61.78, 0.00469	50, 0.02148	61.34, 0.012
Crossplane_450	99.58, 0.00205	99.58, 0.00027	100 , 0.01072	99.58, 0.00123	96.45, 0.01278	100 , 0.00851
Crossplane_500	100 , 0.00216	100 , 0.00031	100 , 0.00758	100 , 0.0019	100 , 0.01092	100 , 0.00734
Average AUC(%), Average time(s)	58.12, 0.00405	57.98, 0.00031	60.01, 0.0113	61.53, 0.00406	62.46 , 0.01766	61.58, 0.01225

freedom (5, 105), as there are six algorithms and 22 datasets involved. Considering a significance level of $\alpha = 0.05$, the critical value for $F(5, 105)$ is 2.30. Since the computed value of F_F is 10.99, which exceeds the critical value of 2.30, we reject the null hypothesis. Additionally, we conducted the Nemenyi post-hoc test to perform pairwise comparisons between the algorithms. The CD is calculated at a significance level of $p = 0.10$ and should exhibit a minimum difference of 1.46 to indicate a significant distinction between the algorithms, clearly seen in Fig. (7).

4.5. Influence of energy parameters E_1 and E_2 on proposed models

To examine the influence of energy parameters E_1 and E_2 on the performance of our IF-RELSTSV and F-RELSTSV, we conducted experiments using the Ecoli-0-3-4-7_vs_5-6 and Yeast3 datasets. The hyperplane must be positioned at a distance of unity from points of other classes in LTSVM, increasing its sensitivity to outliers. However, our IF-RELSTSV and F-RELSTSV introduce energy terms, E_1 and E_2 for each hyperplane similar to ELS-TSVM. By selecting suitable values for these parameters through grid search within the range $[0.6, 0.7, 0.8, 0.9, 1.0]$, we can reduce the sensitivity of the classifier to noise, thereby improving its effectiveness and robustness. The energy parameters E_1 and E_2 are chosen such that the certainty of sample classification in either class is equal. If the E_1/E_2 ratio is large, it indicates a

Table 6 Rank comparison on synthetic datasets with linear kernel.

DATASETS	LSTSVM [12]	ELS-TSVM [14]	IFLSTSVM [17]	RELS-TSVM [15]	Proposed IF-RELSTSVM	Proposed F-RELSTSVM
03subcl5-600-5-0-BI	5.5	5.5	4	2	3	1
03subcl5-600-5-30-BI	5	3	6	1	2	4
03subcl5-600-5-50-BI	4	5	6	3	1	2
03subcl5-600-5-70-BI	4.5	4.5	6	3	2	1
03subcl5-800-7-0-BI	5	4	6	2	1	3
03subcl5-800-7-30-BI	5	6	4	1	2	3
03subcl5-800-7-50-BI	5	4	6	1	2	3
03subcl5-800-7-60-BI	5	6	4	2	1	3
03subcl5-800-7-70-BI	6	4	5	1	3	2
04clover5z-600-5-30-BI	3	5	2	6	1	4
04clover5z-600-5-50-BI	5	6	2	3	1	4
04clover5z-600-5-60-BI	2	4.5	3	4.5	6	1
04clover5z-800-7-30-BI	6	4.5	2	4.5	1	3
04clover5z-800-7-50-BI	3	6	1	4	2	5
04clover5z-800-7-60-BI	2	3	1	4	5	6
04clover5z-800-7-70-BI	5	5	1	5	2	3
Paw02a-600-5-0-BI	4	4	4	2	1	6
Paw02a-600-5-30-BI	3	4	1	5	6	2
Paw02a-800-7-0-BI	5	3	6	2	4	1
Paw02a-800-7-30-BI	5	4	1	2	6	3
Crossplane_450	4	4	1.5	4	6	1.5
Crossplane_500	3.5	3.5	3.5	3.5	3.5	3.5
Average rank	4.34	4.48	3.45	2.98	2.8	2.95

Table 7 Performance comparison on synthetic datasets with Gaussian kernel.

DATASETS	LSTSVM [12]	ELS-TSVM [14]	IFLSTSVM [17]	RELS-TSVM [15]	Proposed IF-RELSTSVM	Proposed F-RELSTSVM
	AUC(%), Time(s)	AUC(%), Time(s)	AUC(%), Time(s)	AUC(%), Time(s)	AUC(%), Time(s)	AUC(%), Time(s)
03subcl5-600-5-0-BI	83.36, 0.03875	83.36, 0.03056	73.99, 0.05803	92.95, 0.06509	93.03, 0.09131	93.62 , 0.10386
03subcl5-600-5-30-BI	75, 0.04434	77.58, 0.02795	66.39, 0.04901	74.96, 0.06601	81.97 , 0.06768	75, 0.09756
03subcl5-600-5-50-BI	71.83, 0.03484	67.69, 0.02306	58.57, 0.04374	73.02, 0.056	75.93 , 0.07242	75.8, 0.09662
03subcl5-600-5-70-BI	61.7, 0.037	68.24, 0.02766	61.36, 0.04807	73.99, 0.05576	69.81, 0.07851	74.7 , 0.10413
03subcl5-800-7-0-BI	83.86, 0.0679	79.97, 0.05103	71.28, 0.07249	92.43, 0.11963	93.12 , 0.14713	92.2, 0.18821
03subcl5-800-7-30-BI	81.4 , 0.07534	64.96, 0.05484	64.63, 0.08307	74.87, 0.13442	73.85, 0.15249	74.18, 0.19493
03subcl5-800-7-50-BI	70.7, 0.06712	66.64, 0.0558	53.76, 0.07817	76.92 , 0.11743	74.31, 0.14087	75.54, 0.18732
03subcl5-800-7-60-BI	74.51, 0.06824	57.74, 0.05845	65.65, 0.07365	76.63, 0.12002	71.62, 0.13055	78.24 , 0.19097
03subcl5-800-7-70-BI	63.41, 0.06906	59.46, 0.05118	51.35, 0.06581	69.58, 0.12281	62.85, 0.12686	73.82 , 0.19475
04clover5z-600-5-30-BI	92.02 , 0.02988	78.63, 0.02694	76.31, 0.03289	85.14, 0.0527	84.71, 0.05968	89.53, 0.08698
04clover5z-600-5-50-BI	67.4, 0.03458	73.48, 0.02866	64.82, 0.03425	78.63, 0.0557	76.22, 0.06151	79.43 , 0.08919
04clover5z-600-5-60-BI	79.05 , 0.03482	54.39, 0.02666	60.47, 0.03473	68.67, 0.05609	62.8, 0.06062	77.91, 0.09168
04clover5z-800-7-30-BI	78.43 , 0.07276	67.82, 0.05407	68.87, 0.06971	75.34, 0.12518	78.23, 0.1621	69.3, 0.19545
04clover5z-800-7-50-BI	73.56 , 0.07542	57.74, 0.05455	62.68, 0.07012	66.18, 0.13582	71.12, 0.14211	69.84, 0.20474
04clover5z-800-7-60-BI	62.19, 0.06764	56.03, 0.05498	58.34, 0.07491	65.49, 0.12321	67, 0.13505	69.61 , 0.19664
04clover5z-800-7-70-BI	63.21, 0.06764	50.76, 0.05412	56.39, 0.07267	59.76, 0.12286	65.95 , 0.13424	64.34, 0.19374
Paw02a-600-5-0-BI	96.41, 0.02145	98.65 , 0.02048	93.96, 0.03468	94.93, 0.04034	96.96, 0.04603	96.96, 0.06236
Paw02a-600-5-30-BI	70.35, 0.02495	83.78, 0.02155	84.59 , 0.03316	82.73, 0.04146	84.33, 0.05043	81.97, 0.06953
Paw02a-800-7-0-BI	96.08 , 0.05678	94.73, 0.04067	95.42, 0.06393	95.75, 0.08512	95.29, 0.10425	95.75, 0.13335
Paw02a-800-7-30-BI	79.06, 0.05723	79.38, 0.04313	72.3, 0.0627	84.16, 0.08904	88.31 , 0.1052	76.29, 0.14396
Crossplane_450	99.58, 0.00588	100 , 0.00558	100 , 0.01774	100 , 0.0126	99.58, 0.0241	99.58, 0.01883
Crossplane_500	96.88, 0.01796	100 , 0.00677	100 , 0.01843	100 , 0.01713	100 , 0.02427	100 , 0.02325
Average AUC(%), Average time(s)	78.18, 0.04862	73.68, 0.03721	70.96, 0.05418	80.1, 0.08247	80.32, 0.09625	81.07 , 0.13037

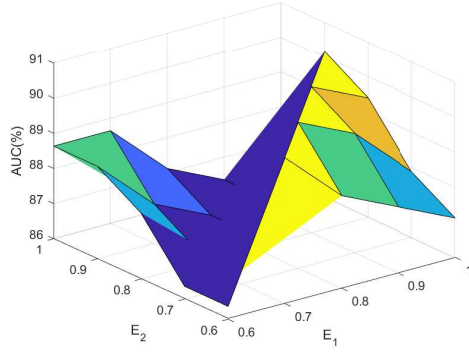
Table 8 Rank comparison on synthetic datasets with Gaussian kernel.

DATASETS	LTSVM [12]	ELS-TSVM [14]	IFLTSVM [17]	RELS-TSVM [15]	Proposed IF-RELSTSV	Proposed F-RELSTSV
03subcl5-600-5-0-BI	4.5	4.5	6	3	2	1
03subcl5-600-5-30-BI	3.5	2	6	5	1	3.5
03subcl5-600-5-50-BI	4	5	6	3	1	2
03subcl5-600-5-70-BI	5	4	6	2	3	1
03subcl5-800-7-0-BI	4	5	6	2	1	3
03subcl5-800-7-30-BI	1	5	6	2	4	3
03subcl5-800-7-50-BI	4	5	6	1	3	2
03subcl5-800-7-60-BI	3	6	5	2	4	1
03subcl5-800-7-70-BI	3	5	6	2	4	1
04clover5z-600-5-30-BI	1	5	6	3	4	2
04clover5z-600-5-50-BI	5	4	6	2	3	1
04clover5z-600-5-60-BI	1	6	5	3	4	2
04clover5z-800-7-30-BI	1	6	5	3	2	4
04clover5z-800-7-50-BI	1	6	5	4	2	3
04clover5z-800-7-60-BI	4	6	5	3	2	1
04clover5z-800-7-70-BI	3	6	5	4	1	2
Paw02a-600-5-0-BI	4	1	6	5	2.5	2.5
Paw02a-600-5-30-BI	6	3	1	4	2	5
Paw02a-800-7-0-BI	1	6	4	2.5	5	2.5
Paw02a-800-7-30-BI	4	3	6	2	1	5
Crossplane_450	5	2	2	2	5	5
Crossplane_500	6	3	3	3	3	3
Average rank	3.36	4.48	5.09	2.84	2.7	2.52

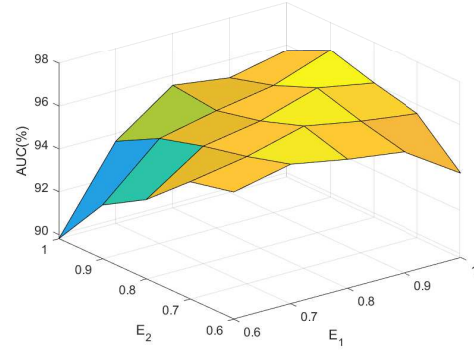
higher certainty for the sample to belong to one class over the other, and vice versa. Figs. (8a) and (8b) showcase the impact of energy parameters E_1 and E_2 for classifying the Ecoli-0-3-4-7_vs_5-6 and Yeast3 datasets. Fig. (8a) illustrates that IF-RELSTSV performs better on the Ecoli-0-3-4-7_vs_5-6 dataset when E_1 and E_2 values are comparable. Similarly, Fig. (8b) demonstrates that the proposed IF-RELSTSV achieves better performance on Yeast3 with higher E_1 values and lower E_2 values, indicating the classifier's ability to adjust and reduce sample sensitivity. Likewise, Fig. (9a) and (9b) reveal improved performance on both the Ecoli-0-3-4-7_vs_5-6 and Yeast3 datasets respectively, with higher E_1 values and lower E_2 values. Notably, the performance of the F-RELSTSV fluctuates as E_1 and E_2 values vary, reflecting the adaptive nature of the hyperplane, and its tendency to optimize energy values for better noise handling.

5. Credit card fraud detection

To show the application of the proposed algorithms on real world problems, we take the credit card fraud detection dataset [30, 31] of large size and with a high imbalance ratio.

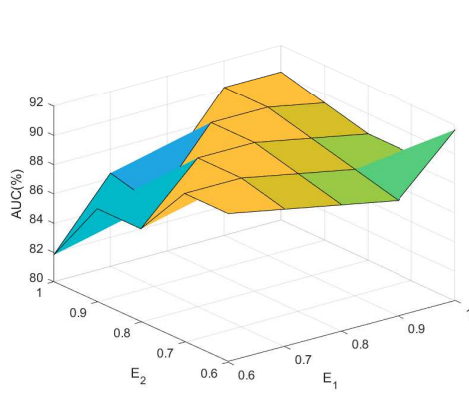


(a) Ecoli-0-3-4-7_vs_5-6

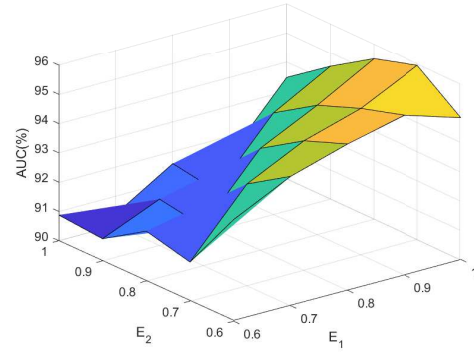


(b) Yeast3

Figure 8: Performance of IF-RELSTSVM on energy parameters (E_1 , E_2) for Ecoli-0-3-4-7_vs_5-6 and Yeast3 datasets



(a) Ecoli-0-3-4-7_vs_5-6



(b) Yeast3

Figure 9: Performance of F-RELSTSVM on energy parameters (E_1 , E_2) for Ecoli-0-3-4-7_vs_5-6 and Yeast3 datasets

Table 9 Performance on credit card fraud detection.

DATASETS	LTSVM [12]	ELS-TSVM [14]	IFLTSVM [17]	RELS-TSVM [15]	Proposed IF-RELSTSVM	Proposed F-RELSTSVM
Creditcard_10K	85.42, 0.50347	85.42, 0.09123	85.42, 1.02423	85.42, 0.68781	89.35, 1.85272	91.56 , 14.6528
Creditcard_20K	74.48, 2.2466	74.48, 0.00341	74.48, 7.81414	74.48, 3.58598	91.69, 12.6311	92.79 , 9.42395
Creditcard_30K	74.95, 6.27077	72.97, 0.0044	72.97, 16.6391	72.97, 10.5538	86.94 , 32.5731	85.43, 27.1823
Creditcard_40K	75.38, 16.9848	74.56, 0.00462	75.38, 28.8133	74.56, 29.7912	88.69, 93.1857	90.51 , 80.3976
Creditcard_50K	78.61, 48.0747	78.62, 0.0113	78.61, 86.9384	78.62, 66.0247	92.43, 279.209	93.9 , 256.628
Average AUC(%), Average time(s)	77.77, 14.81607	77.21, 0.02299	77.37, 28.24583	77.21, 22.1287	89.82, 83.89032	90.84 , 77.65693

In the preprocessing, we performed PCA transformation on the features. Therefore, the datasets contain features from V_1, V_2, \dots, V_{28} as the principal components. The time and amount features are excluded from the PCA analysis. We include the amount feature later as the amount feature is used for dependent cost-sensitive learning. As datasets are large so we take datasets of different sizes viz. 10K, 20K, 30K, 40K, and 50K. The training size is 60% of total samples, and chosen fixed value for C_1, C_2, C_3, C_4 as 1, and E_1 and E_2 is set as 0.8 using linear kernel. The proposed IF-RELSTSVM and F-RELSTSVM outperform on credit card fraud detection dataset as we can see in Table 9. The average AUC of proposed IF-RELSTSVM and F-RELSTSVM are 89.82% and 90.84% respectively, followed by LTSVM with 77.77%, IFLTSVM with 77.37%, and both ELS-TSVM and RELS-TSVM achieve 77.21%. This demonstrates that our proposed algorithms IF-RELSTSVM and F-RELSTSVM perform better than the baseline algorithms.

6. Conclusions

This study proposes novel and enhanced versions of the RELS-TSVM model using fuzzy membership values. To deal with the class imbalance and noise simultaneously, we presented a projection based fuzzy membership assignment (PFMA), and used in our proposed robust fuzzy energy-based least square twin support vector machine (F-RELSTSVM). The proposed algorithm deals with noise present near and away from the hyperplane by using the fusion of energy and projection based approaches. The proposed F-RELSTSVM also involves the 2-norm of the slack variable to ensure strong convexity in the optimization problem.

Moreover, we also propose another enhanced version of RELS-TSVM, by using a well-known fuzzy membership technique i.e. intuitionistic fuzzy membership to propose IF-RELSTSVM. This ensures that the optimization problems in IF-RELSTSVM remain insensitive to noise and outliers. Based on the

experimental results, it can be concluded that the proposed F-RELSTSVM demonstrates strong generalization performance, particularly in noisy data, surpassing the baseline algorithms. Furthermore, we showed the application of the proposed F-RELSTSVM on credit card fraud detection, where the proposed F-RELSTSVM outperformed all the other baseline algorithms. This justifies the applicability of the proposed algorithm in real world scenarios.

In future, we aim to improve the selection process for getting the proximal plane in the proposed fuzzy membership degree by exploring heuristic-based approaches that will reduce training time. Extending our approach to handle multi-class classification problems is an exciting avenue for further investigation.

References

- [1] Corinna Cortes and Vladimir Vapnik. Support-vector networks. *Machine Learning*, 20:273–297, 1995.
- [2] M Tanveer, Bharat Richhariya, Riyaj Uddin Khan, Ashraf Haroon Rashid, Pritee Khanna, Mukesh Prasad, and CT Lin. Machine learning techniques for the diagnosis of alzheimer’s disease: A review. *ACM Transactions on Multimedia Computing, Communications, and Applications (TOMM)*, 16(1s):1–35, 2020.
- [3] Richard G Brereton and Gavin R Lloyd. Support vector machines for classification and regression. *Analyst*, 135(2):230–267, 2010.
- [4] Latifur Khan, Mamoun Awad, and Bhavani Thuraisingham. A new intrusion detection system using support vector machines and hierarchical clustering. *The VLDB Journal*, 16:507–521, 2007.
- [5] Bharat Richhariya and Deepak Gupta. Facial expression recognition using iterative universum twin support vector machine. *Applied Soft Computing*, 76:53–67, 2019.
- [6] Michael Schmidt and Herbert Gish. Speaker identification via support vector classifiers. In *1996 IEEE International Conference on Acoustics, Speech, and Signal Processing Conference Proceedings*, volume 1, pages 105–108. IEEE, 1996.

- [7] Bo-Feng Zhang, Jin-Shu Su, and Xin Xu. A class-incremental learning method for multi-class support vector machines in text classification. In *2006 International Conference on Machine Learning and Cybernetics*, pages 2581–2585. IEEE, 2006.
- [8] Bharat Richhariya and Muhammad Tanveer. EEG signal classification using universum support vector machine. *Expert Systems with Applications*, 106:169–182, 2018.
- [9] Rukshan Batuwita and Vasile Palade. FSVM-CIL: Fuzzy support vector machines for class imbalance learning. *IEEE Transactions on Fuzzy Systems*, 18(3):558–571, 2010.
- [10] Shiliang Sun, Xijiong Xie, and Chao Dong. Multiview learning with generalized eigenvalue proximal support vector machines. *IEEE Transactions on Cybernetics*, 49(2):688–697, 2018.
- [11] Jayadeva, Reshma Khemchandani, and Suresh Chandra. Twin support vector machines for pattern classification. *IEEE Transactions on Pattern Analysis and Machine Intelligence*, 29(5):905–910, 2007.
- [12] M. Arun Kumar and M. Gopal. Least squares twin support vector machines for pattern classification. *Expert Systems with Applications*, 36(4):7535–7543, 2009. ISSN 0957-4174.
- [13] Qi Wang, Yue Ma, Kun Zhao, and Yingjie Tian. A comprehensive survey of loss functions in machine learning. *Annals of Data Science*, pages 1–26, 2020.
- [14] Jalal A Nasiri, Nasrollah Moghadam Charkari, and Kourosh Mozafari. Energy-based model of least squares twin support vector machines for human action recognition. *Signal Processing*, 104:248–257, 2014.
- [15] Mohammad Tanveer, Mohammad Asif Khan, and Shen-Shyang Ho. Robust energy-based least squares twin support vector machines. *Applied Intelligence*, 45:174–186, 2016.
- [16] Muhammad Tanveer, Chandan Gautam, and Ponnuthurai N Suganthan. Comprehensive evaluation of twin svm based classifiers on uci datasets. *Applied Soft Computing*, 83:105617, 2019.

- [17] Scindhiya Laxmi, SK Gupta, and Sumit Kumar. Intuitionistic fuzzy least square twin support vector machines for pattern classification. *Annals of Operations Research*, pages 1–50, 2022.
- [18] Krassimir T Atanasov. *Intuitionistic fuzzy sets*. Springer, 1999.
- [19] Harsurinder Kaur, Husanbir Singh Pannu, and Avleen Kaur Malhi. A systematic review on imbalanced data challenges in machine learning: Applications and solutions. *ACM Computing Surveys (CSUR)*, 52(4): 1–36, 2019.
- [20] B. Richhariya and M. Tanveer. A robust fuzzy least squares twin support vector machine for class imbalance learning. *Applied Soft Computing*, 71:418–432, 2018.
- [21] Bharat Richhariya and Muhammad Tanveer. A reduced universum twin support vector machine for class imbalance learning. *Pattern Recognition*, 102:107150, 2020.
- [22] Jin Huang and Charles X Ling. Using AUC and accuracy in evaluating learning algorithms. *IEEE Transactions on Knowledge and Data Engineering*, 17(3):299–310, 2005.
- [23] L.A. Zadeh. Fuzzy sets. *Information and Control*, 8(3):338–353, 1965. ISSN 0019-9958.
- [24] Minghu Ha, Chao Wang, and Jiqiang Chen. The support vector machine based on intuitionistic fuzzy number and kernel function. *Soft Computing*, 17:635–641, 2013.
- [25] Gene H Golub and Charles F Van Loan. *Matrix computations*. JHU press, 2013.
- [26] J Derrac, S Garcia, L Sanchez, and F Herrera. Keel data-mining software tool: Data set repository, integration of algorithms and experimental analysis framework. *J. Mult. Valued Logic Soft Comput*, 17, 2015.
- [27] Krystyna Napierała, Jerzy Stefanowski, and Szymon Wilk. Learning from imbalanced data in presence of noisy and borderline examples. In *Rough Sets and Current Trends in Computing: 7th International Conference, RSCTC 2010, Warsaw, Poland, June 28-30, 2010. Proceedings* 7, pages 158–167. Springer, 2010.

- [28] Janez Demšar. Statistical comparisons of classifiers over multiple data sets. *The Journal of Machine Learning Research*, 7:1–30, 2006.
- [29] Yuan-Hai Shao, Chun-Hua Zhang, Xiao-Bo Wang, and Nai-Yang Deng. Improvements on twin support vector machines. *IEEE Transactions on Neural Networks*, 22(6):962–968, 2011.
- [30] Andrea Dal Pozzolo, Giacomo Boracchi, Olivier Caelen, Cesare Alippi, and Gianluca Bontempi. Credit card fraud detection: A realistic modeling and a novel learning strategy. *IEEE Transactions on Neural Networks and Learning Systems*, 29(8):3784–3797, 2017.
- [31] Bertrand Leblot, Yann-Aël Le Borgne, Liyun He-Guelton, Frederic Oblé, and Gianluca Bontempi. Deep-learning domain adaptation techniques for credit cards fraud detection. In *Recent Advances in Big Data and Deep Learning: Proceedings of the INNS Big Data and Deep Learning Conference INNSBDDL2019, held at Sestri Levante, Genova, Italy 16-18 April 2019*, pages 78–88. Springer, 2020.